Preprints of the 21st IFAC World Congress (Virtual)
Berlin, Germany, July 12-17, 2020

On Expressive Features for Gait Analysis using Lower Limb Inertial Sensor Data

Felix Laufer * **Michael Lorenz** * **Bertram Taetz** *
Gabriele Bleser *

* *Technische Universität Kaiserslautern, Kaiserslautern, Germany (e-mail: {surname}@cs.uni-kl.de).*

Abstract: In this paper, we present a method to obtain explicit, expressive and interpretable gait feature signals from an inertial sensor, mounted on any segment of the lower limbs. The proposed method is invariant to the mounting orientation of the sensor, works without magnetometer information, requires no prior knowledge and can be used in real-time scenarios. Moreover, the constructed signals are robust for a wide variety of changing walking speeds and directions. We investigate the informational content of our three feature signals lying in the human sagittal plane with respect to the gait phase segmentation problem and compare them to other commonly used signals, such as the sagittal angular velocity and the norms of accelerations and angular velocities. To this end, we make use of the filter-based maximum relevance minimum redundancy algorithm, which is a classifier-independent feature selection method. For validating our approach, we consider gait data of twelve healthy subjects walking straight and in curves at self-chosen speeds with inertial sensors attached to either the thigh, shank or foot. Additionally, pressure measuring insoles are used to obtain ground truth toe-off and heel-strike gait events for reference. With those events as the gait phase transitions, the event detection is cast into a classification problem. To support the theoretical findings of the feature selection and ranking, we finally evaluate different choices of feature sets with a simple linear support vector machine classifier in an online fashion and obtain superior segmentation results with our feature signals.

Keywords: Gait segmentation, bio-signals analysis and interpretation, human body motion capture, information and sensor fusion, motion estimation, parameter and state estimation, inertial sensors, signal processing, machine learning

1. INTRODUCTION

Inertial measurement units (IMUs) are nowadays used for many on-body scenarios and mostly comprise three-axis gyroscopes, accelerometers and sometimes magnetometers. The microelectromechanical systems (MEMS) technology allows to construct them in a small, lightweight and low-energy consuming manner, which facilitates an easy attachment on the human body. As pointed out in Aminian et al. (2002), this might be one of the major reasons, why they emerged in various fields of application such as sports, rehabilitation or daily life monitoring over the past decade.

Particularly in the field of human gait analysis, MEMS IMUs proved to deliver reliable results. Many publications show that gait segmentation and event detection relying on inertial data works fairly well. An overview of existing gait analysis methods, using IMUs and adaptive algorithms, is given in Caldas et al. (2017).
To detect gait phases, IMUs are typically attached to the feet, shanks or thighs. Methods for biomedical gait analysis applications based on sensors, attached to the thighs or shanks, are presented in Kotiadis et al. (2010), Bötzel et al. (2016), Maqbool et al. (2017) and Abhayasinghe and Murray (2014).
Algorithms to detect different gait phases from a foot-worn inertial sensor are proposed f.i. by Seel et al. (2014), Mariani et al. (2013), Rueterbories et al. (2014), Mannini et al. (2014) and Schicketmueller et al. (2019).
In the context of indoor positioning, an IMU can be integrated into a shoe to detect gait phases as done by Kim et al. (2014) and Wang et al. (2015).
All aforementioned approaches have the common disadvantage that they cannot be easily ported from one limb to the other, without the effort of additional adaptions.
Solutions to overcome this are addressed by the work of Guenterberg et al. (2009), Aung et al. (2013) and Taborri et al. (2014). They present approaches based on learned Hidden Markov Models, which can be used with sensors, that are attached arbitrarily on the lower limbs or even the upper body after a training phase, but are hence dependent on data sets.

In order to comprehend the basic idea of the work introduced above, one might ask, where and how the most relevant information for inertial gait segmentation is encoded — particularly in view of the heuristic, but also the data-driven learning approaches.
Fig. 1 illustrates the human body planes and axis. During the normal gait cycle, the predominant motion in the lower limbs in terms of absolute ranges of motion is contained within the sagittal plane. When walking straight, flexion-

extension occurs at the ankle, knee and hip and the related joint axes are approximately coincident with the mediolateral axis, as discussed in the work of Perry and Burnfield (2010).
Studying the related work, it can be summarized that segmentation methods, using gyroscope or accelerometer data, mainly exploit sagittal information. In particular, three complementary and orthogonal signal components can be identified from literature and appear to be most relevant:

(1) sagittal angular velocity,
(2) accelerations in anteroposterior direction,
(3) vertical accelerations, esp. when the foot strikes and lifts off the ground.

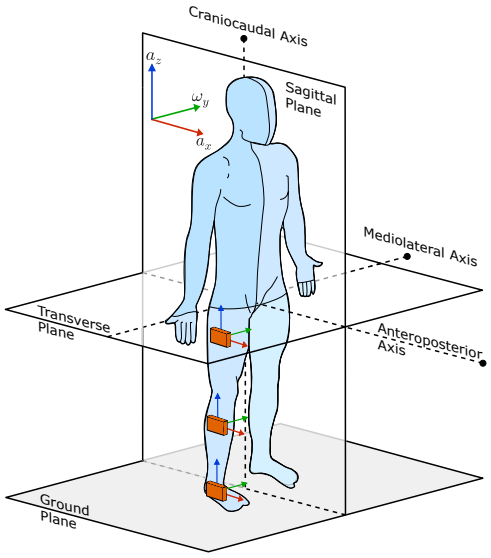

Fig. 1. Anatomical human body planes, cf. Wikimedia Commons (2014). Sensors at the lower limbs are aligned with a coordinate frame composed of the three body axes, which coincide with the directions of the relevant gait signal components a_x, ω_y and a_z.

Most of the heuristic methods directly use one or more of these signals as done e.g. in Wang et al. (2015), Mariani et al. (2013) and Schicketmueller et al. (2019). Some derive closely related features from the signals as done by Seel et al. (2014) or Kotiadis et al. (2010).

We assume that during normal gait, an IMU mounted to any lower limb segment measures most of the signal variance related to progressive motion within the sagittal plane. The remaining components might be merely superimposed with additional accelerations and angular velocities due to changes of the heading direction, when walking in curves, or caused by pathological gait deviations, soft tissue and clothing artifacts.
Supposing a favorable sensor alignment with the IMU's y-axis parallel with the mediolateral axis and its z-axis pointing opposed to the gravity vector, the three most relevant gait signals would be given by the sensor measurements immediately, cf. Fig. 1. The contiguous inertial time series of the aforementioned components, measured at any lower limb segment, are hereinafter referred to as the three (gait) feature signals. This term is intended to distinguish these intuitively interpretable signals from more abstract, implicit or hidden features, appearing in the context of machine learning and automatic feature extraction in particular. However, in context of the introduced approaches from literature, obtaining these signals either requires a fixed and invariant sensor mounting w.r.t. the respective limb, prior knowledge of the sensor-to-segment alignment or an entangled learning process of the alignment, along with some implicit features.

In contrast to existing work, our proposed approach is independent of prior knowledge, while still exploiting the sagittal information for all lower limbs explicitly. Moreover, our proposed method is independent from a laboratory environment and can be used for arbitrary walking directions and a wide range of speeds.
In summary, the contributions of this work are:

- Construction and online tracking of informative features, aligned with sagittal and ground plane, without using magnetometers at any time.
- Comparison to commonly used features, regarding predictive power and information gain.
- Evaluation of features for online gait segmentation, using common classifiers.

2. METHOD

Fig. 2 illustrates the overall methodology of obtaining and evaluating our proposed gait feature signals. Each of the following sections corresponds to a box in the figure and will be discussed in detail subsequently.
Finally, the data recording and processing is described.

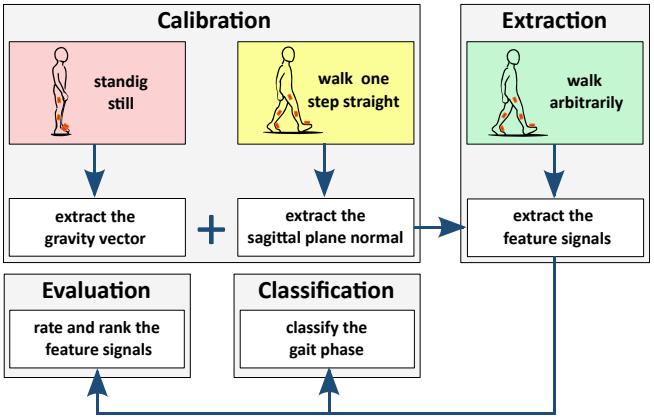

Fig. 2. Schematic illustration of the proposed gait feature signal methodology.

Notation The processing method of the gait feature signals was the same for any lower limb IMU. Therefore, the coordinate frame of an IMU is denoted by I and assumed to be aligned with the sensor casings at the foot, shank or thigh, respectively. Accelerations and angular velocities are $a, \omega \in \mathbb{R}^3$ and g is the local gravity constant. The estimated gravitational direction and sagittal plane normal are denoted by $\hat{g}$ and $\hat{s} \in \mathbb{R}^3$. The angular velocity and acceleration frames, after applying some initial rotations for sensor-to-segment alignment, are denoted S_ω and S_a. The acceleration frame after an additional rotation for inclination compensation is denoted $\bar{S}_a$ and G is the inertial frame of reference. A rotation matrix $R^{AB} \in \mathbb{R}^{3\times3}$ rotates a three dimensional vector from frame B to A.

2.1 Calibration

As a first step to obtain pure sagittal inertial data, an initial transformation is required, which rotates the sensor from its unknown mounting orientation into a segment-aligned coordinate frame. For estimating this rotation matrix, a two-staged calibration phase was performed, where measurements during a quasi-static standing pose and afterwards a dynamic sequence of one step in walking direction, were collected.

Estimating the Ground Plane Normal For estimating the gravitational direction, i.e. the normal of the ground plane, a set of IMU measurements was required to fulfill the following conditions of a quasi-static sensor pose:

$$||a^I||_2 - g \leq \tau_a, \tag{1a}$$

$$||\omega^I||_2 \leq \tau_\omega\,, \tag{1b}$$

with some small thresholds τ_a, τ_ω.
These accelerations during static conditions were aggregated in $A \in \mathbb{R}^{n\times 3}$ with n the number of static pose measurements. Then the column-wise mean of A was computed and normalized, yielding the desired gravitational direction $\hat{g}^I$ in the inertial sensor frame.

Estimating the Sagittal Plane Normal In a second calibration stage, the subject was expected to take a step in walking direction with the leg, where the considered sensor was attached to. This process was started when both conditions in Eq. 1 were invalidated and stopped as soon as they evaluated true again. We aggregated the angular velocities during the supposed step in $\Omega \in \mathbb{R}^{n\times 3}$, with n the number of measurements. As a precaution to remove any potential gyroscope biases, we centered the data by subtracting the column-wise means from each row yielding $\bar{\Omega}$. We then applied a principal component analysis (PCA) on $\bar{\Omega}$ implemented via singular value decomposition, cf. Jolliffe (2002). The first principal component gave us an estimate of the desired local sagittal normal $\hat{s}^I$ in the inertial sensor frame.
Note, that the PCA is ambiguous in terms of the sign of a principal component. Hence, the collected data was projected onto $\hat{s}^I$, the first significant local extremum of the resulting signal was checked and $\hat{s}^I$ was inverted in case of a minimum. After that, $\hat{s}^I$ formed a right-handed coordinate frame together with $-\hat{g}^I$ and the positive walking direction.
All further incoming gyroscope measurements ω_t^I could then be likewise projected and yielded the sagittal angular velocity component of the desired gait feature signal:

$$\omega_{t,y}^{S_\omega} = \omega_t^I \cdot \hat{s}^I\,. \tag{2}$$

2.2 Extraction

In order to continuously extract the gait feature signals in an online fashion, the previously estimated ground and sagittal axes were used to construct the initial rotation matrix. This allows to transform the sensor measurements into a known, segment-aligned coordinate frame with its x-y-plane parallel to the ground with regard to a neutral standing pose.

Pre-rotating the Measurements The initial rotation matrix R^{SaI} was constructed based on $\hat{g}^I$ and $\hat{s}^I$:

$$R^{S_aI} = \begin{pmatrix} \left(\hat{s}^I \times -\hat{g}^I\right)^T \\ \left(-\hat{g}^I \times \left(\hat{s}^I \times -\hat{g}^I\right)\right)^T \\ \left(-\hat{g}^I\right)^T \end{pmatrix} \tag{3}$$

Note, that the local sagittal normal $\hat{s}^I$, technically speaking the estimate of the limb's mediolateral axis, is not necessarily orthogonal to $\hat{g}^I$. In respect of proper anteroposterior and vertical accelerations, the z-axis of the segment-aligned acceleration frame was forced to coincide with gravity and hence $\hat{s}^I$ was not used as the y-basis of R^{S_aI}.
The incoming sensor measurements were finally be pre-rotated:

$$a_t^{S_a} = R^{S_aI}\, a_t^I\,, \tag{4a}$$

$$\omega_t^{S_a} = R^{S_aI}\, \omega_t^I\,. \tag{4b}$$

Tracking the Inclination Subsequently, the sensor inclination was estimated over time, using an extended Kalman filter (EKF), which allowed for a compensation of the time-dependent variations in orientation in the roll and pitch directions. This way, the accelerometer measurements could be rotated into a frame, aligned with the sagittal and ground plane, thus yielding pure vertical and anteroposterior accelerations in the x and z-components. The aforementioned pre-rotation of the measurements allowed for an initialization of the roll-pitch tracking with a zero-inclination guess, reducing the initial settling time and also avoiding a potential Gimbal lock.
Assuming a gravity-dominant acceleration measurement model, the instantaneous roll ϕ_t^G and pitch θ_t^G Euler angles in the inertial frame were estimated from the pre-rotated accelerations $a_t^{S_a}$:

$$\hat{\phi}_{a,t}^G = \arctan\left(\frac{a_{t,y}^{S_a}}{\sqrt{\left(a_{t,x}^{S_a}\right)^2 + \left(a_{t,z}^{S_a}\right)^2}}\right), \tag{5a}$$

$$\hat{\theta}_{a,t}^G = \arctan\left(\frac{a_{t,x}^{S_a}}{\sqrt{\left(a_{t,y}^{S_a}\right)^2 + \left(a_{t,z}^{S_a}\right)^2}}\right). \tag{5b}$$

The instantaneous Euler rates of change of roll and pitch $\dot{\phi}_{\omega,t}^G, \dot{\theta}_{\omega,t}^G$ can be expressed in the inertial frame depending on the previous segment inclination and the pre-rotated angular velocity measurements as follows, cf. Gustafsson (2012):

$$\begin{pmatrix} \dot{\phi}_{\omega,t}^G \\ \dot{\theta}_{\omega,t}^G \end{pmatrix} = \begin{pmatrix} 1 & \sin\phi_{t-1}^G \tan\theta_{t-1}^G & \cos\phi_{t-1}^G \tan\theta_{t-1}^G \\ 0 & \cos\phi_{t-1}^G & -\sin\phi_{t-1}^G \end{pmatrix} \omega_t^{S_a} \tag{6}$$

Note, that Eq. 6 is prone to a Gimbal lock when pitch approaches $\pm\pi/2$. However, using the initial pre-rotation, this was not an issue during gait motion. One might want to eliminate this singularity with a quaternion orientation representation.
With the aforementioned relationships, the roll-pitch tracking was implemented in an EKF manner, cf. Gustafsson (2012). The state x_t was tracked using the roll and pitch rates of change from Eq. 6 as inputs u_t and the roll and pitch estimates from Eq. 5 as measurements y_t:

$$x_t = \left(\phi_t^G \; b_{\phi,t}^G \; \theta_t^G \; b_{\theta,t}^G\right)^T, \tag{7a}$$

$$u_t = \left(\dot{\phi}_{\omega,t}^G \; \dot{\theta}_{\omega,t}^G\right)^T, \tag{7b}$$

$$y_t = \left(\hat{\phi}_{a,t}^G \; \hat{\theta}_{a,t}^G\right)^T, \tag{7c}$$

with $b_{\phi,t}^G, b_{\theta,t}^G$ the gyroscope biases related to roll and pitch at time t.
The state and measurement equations were then defined in state-space form:

$$x_t = \begin{pmatrix} 1 & -T & 0 & 0 \\ 0 & 1 & 0 & 0 \\ 0 & 0 & 1 & -T \\ 0 & 0 & 0 & 1 \end{pmatrix} x_{t-1} + \begin{pmatrix} T & 0 \\ 0 & 0 \\ 0 & T \\ 0 & 0 \end{pmatrix} u_t + w_t\,, \tag{8a}$$

$$y_t = \begin{pmatrix} 1 & 0 & 0 & 0 \\ 0 & 0 & 1 & 0 \end{pmatrix} x_t + v_t\,, \tag{8b}$$

where T is the sampling time and $w_t \sim \mathcal{N}(0, Q)$ and $v_t \sim \mathcal{N}(0, R)$ are zero-mean Gaussian processes with some process and measurement noise covariance matrices $Q \in \mathbb{R}^{4\times4}$ and $R \in \mathbb{R}^{2\times2}$.

Compensating the Inclination Using the tracked roll and pitch angles, all incoming pre-rotated acceleration measurements were rotated into an inclination-compensated acceleration frame $\bar{S}_a$, remaining parallel to the ground plane over time:

$$a_t^{\bar{S}_a} = R_y(\theta_t^G) R_x(\phi_t^G)\; a_t^{S_a}\,, \tag{9}$$

with $R_x(\cdot), R_y(\cdot)$ the elemental rotations around the x and y-axis, in the reference frame, respectively.
The final gait feature signal vector $f_t \in \mathbb{R}^3$ is defined with the previously computed sagittal angular velocity signal $\omega_{t,y}^{S_\omega}$ and the x and z-components of the aforementioned inclination-compensated accelerations minus gravity:

$$f_t := \left(a_{t,x}^{\bar{S}_a} \; \omega_{t,y}^{S_\omega} \; a_{t,z}^{\bar{S}_a} - g\right)^T. \tag{10}$$

2.3 Evaluation

The relevance and performance of our proposed gait signals were investigated in respect of a binary stance-swing phase segmentation. For ground truth reference, gait events were obtained from pressure measuring insoles, where toe-off (TO) and heel-strike (HS) events were interpreted as the transitions between stance and swing phases and vice versa.

To state, which of the feature signals, obtained from different limbs, is particularly relevant for the task of gait phase detection, a classifier-independent feature selection method, capable of ranking the features with respect to the discriminative information, is desirable.
Feature selection methods can be roughly grouped into three categories: filter-based methods, wrapper methods and embedding methods. In this work we exploited filter-based methods, which have the advantage of scoring features, based on a proxy measure instead of an error rate, obtained by any specific classifier, cf. Blum and Langley (1997). Moreover, when dealing with $m > 1$ features, it is well known that "the m best independent features are not necessarily the best m features" for a classification task, due to correlation and redundancy, Cover (1974).
The minimum redundancy maximum relevance (mRMR) algorithm, originally proposed in Ding and Peng (2005a), Ding and Peng (2005b), solves this problem, and delivers, given a set of features and target classes, a feature ranking through the amount of relevant information for the class, while optimizing with respect to least redundancy. Several variants of the mRMR method have been proposed, including the mutual information quotient (MIQ), the F-test correlation difference and non-linear extensions, cf. e.g. Ding and Peng (2005a), Vinh et al. (2010), Zhao et al. (2019). We chose the mRMR method as introduced by Ding and Peng (2005b) and implemented in Matlab 2019b.

In literature, the Euclidean norms of accelerations and angular velocities are frequently considered for gait phase detection, since they do not require any decomposition into sagittal components and are independent of the sensor mounting orientation, cf. Mariani et al. (2013), Kim et al. (2014) and Seel et al. (2014).
In order to compare the amount of relevant information of the proposed feature signals with the signal norms, we evaluated subsets of the following extended feature set vector including f:

$$\bar{f}_t := \left(f_t^T \; ||\omega_t^I||_2 \; ||a_t^I||_2 - g\right)^T. \tag{11}$$

2.4 Classification

To finally illustrate the effectiveness for gait phase segmentation, a support vector machine (SVM) classifier with a linear kernel was trained and evaluated in an online walk-forward manner. Since the main goal of this work was to develop and evaluate expressive feature signals, rather than selecting and tweaking a specific classifier, we utilized this simple, but representative classification approach.
The SVM has shown to be a reliable machine learning tool for pattern recognition in human gait, as concluded in the recent review of Figueiredo et al. (2018). In order to exemplify the gain in accuracy and reliability due to the proposed feature signals, we applied a SVM with a linear kernel for gait phase classification.
Determining the current phase, given only the recent time instance of a feature set vector, is not robust due to spurious class transitions as no temporal information is present at all. Maintaining the real-time applicability of our approach, a look-back window of size N was thus introduced and the classification problem was formulated to predict the current class of the gait phase, given a batch of the N recent time instances of a feature set. The gait events were then defined as the transitions between different gait phases.

2.5 Data Recording

We captured the motion of the lower limbs, using six IMUs (MTW Awinda Xsens Technologies BV, Enschede, The Netherlands). The IMUs were attached to the thighs, shanks and feet. In order to obtain ground truth gait segmentation information, we used foot pressure distributions measured with two sensor insoles (Smart Foot Sensor, IEE S.A., Bissen, Luxembourg) and respective data loggers (Dialogg data logger, Envisible, Steinbeis-Forschungszentrum, Chemnitz, Germany). The data loggers of the pressure insole also contained an IMU. For synchronization purposes, both foot IMUs and pressure

data loggers were stacked together in 3D printed mounting brackets, which were then laced to the shoes. The overall setup is shown in Fig. 3 and Fig. 4.

Fig. 3. Subject wearing IMUs (orange), pressure insoles and sensor brackets (white) laced to the shoes.

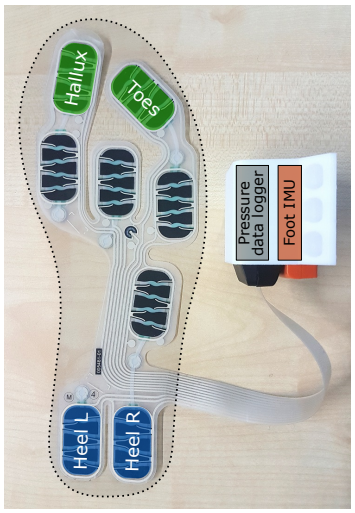

Fig. 4. Eight-channel pressure insole with data logger and foot IMU stacked together in a single shoe-mountable bracket.

Data Synchronization The IMU measurements included each three-axis accelerations and angular velocities and were recorded at a sampling frequency of 60 Hz. The pressure data loggers provided eight-channel pressure data at different regions of the foot and additional accelerations and angular velocities at a sampling frequency of 100 Hz. In order to post-synchronize the recordings of our two systems, we up-sampled the gyroscope measurements of the stacked foot IMUs and pressure data loggers to their least common multiple frequency. After that, the cross-correlation lag of the angular velocity norms was computed over the entire sequence and the pressure data was shifted and re-sampled accordingly, to match the time frame of the IMUs.

Ground Truth Gait Segmentation We investigated two main gait phases: stance and swing as shown in Fig. 5 and obtained our ground truth data, using the pressure insoles consisting of eight force sensing resistor cells, cf. Fig. 4. The method was similar to those mentioned in Storm et al. (2019) and Maqbool et al. (2017). The transitions between both phases were defined as the occurrence of a TO and HS event, respectively. A HS was detected when the sum of pressures at the heel sensor cells, as illustrated in Fig. 4 showed a significant rise. Analogously, a TO event was defined as a fall of the sum of the pressures of the toe and hallux cells.

Collected Data A straight, ground-leveled walking track with a distance of about 8 m was marked with two pylons at the ends. Twelve healthy subjects (two female, ten male) were asked to stand still for a few seconds, walk one straight step for calibration purposes and then follow the track for a period of two minutes, while turning in smooth curves around the pylons. After each turn, the subjects were encouraged to arbitrarily change their walking speeds.
In total, we collected data of 2266 steps with walking speeds ranging from 0.25 m/s to 2.28 m/s, an average speed of 0.98 m/s and a standard deviation of 0.34 m/s.

3. EXPERIMENTAL RESULTS

Computed exemplary gait feature signals for one gait cycle are illustrated in Fig. 5. These signals are qualitatively representative for the evaluated subjects during all walking conditions.

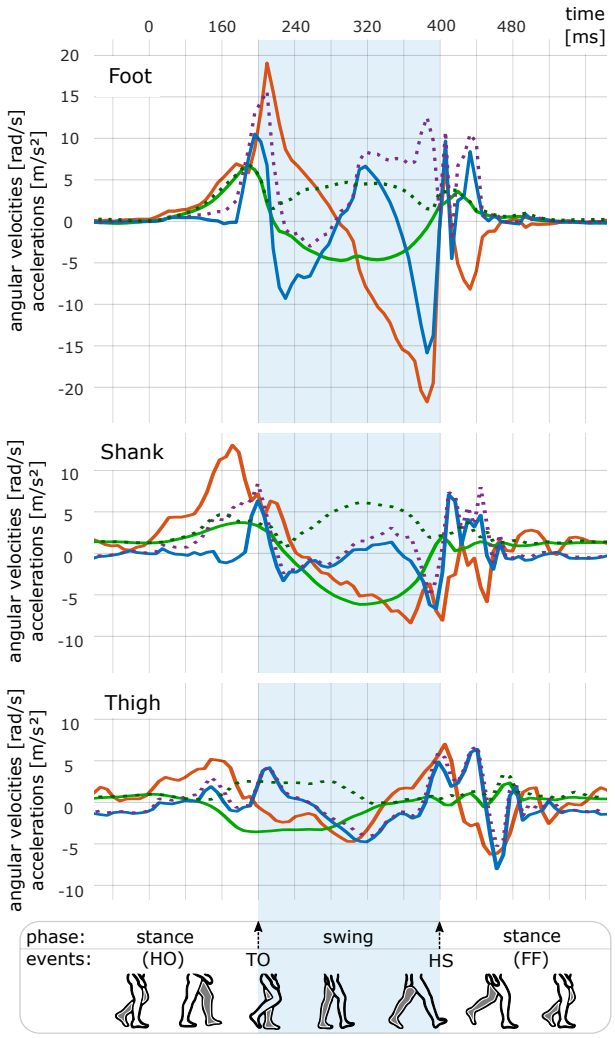

Fig. 5. Exemplary feature signals of each limb segment for one gait cycle: the sagittal angular velocity $\omega_y^{S_\omega}$ (green) and the anteroposterior and vertical accelerations $a_x^{\bar{S}_a}$ (red) and $a_z^{\bar{S}_a}$ (blue). The green dashed lines refer to the norms of the angular velocities (dark green) and accelerations minus gravity (purple).

3.1 Feature Signal Ranking

We ranked different feature subsets, using the mRMR method with respect to the ground truth gait phases. As feature sets, the sagittal angular velocity, our gait feature set vector f, the extended feature set vector $\bar{f}$ including the acceleration and gyroscope norms and the acceleration

and gyroscope norms only were chosen. Only a single time instance of the feature vector, given the labeled class, was used to compute the MIQ, since no significant difference in the score relations has been observed, when a window of N features was used.
Fig. 6 shows the resulting MIQ scores of each feature computed over all subjects and for each limb segment.

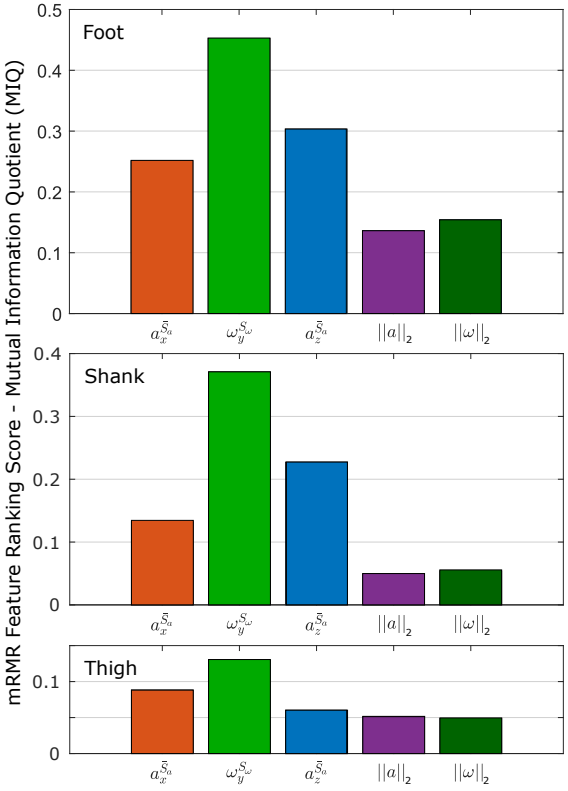

Fig. 6. The mRMR feature ranking and MIQ scores for each feature and each segment computed over the entire data set.

In every case, our three feature signals were ranked higher than the norms of the signals, where the sagittal angular velocity was consistently the most relevant component. The vertical and anteroposterior accelerations still achieved high scores, indicating that they provide relevant additional information.
In case of the foot and shank, the vertical acceleration was chosen as the second most relevant feature in conjunction with the angular velocity, whereas the anteroposterior acceleration was preferred for the thigh. Particularly for the foot and shank, the scores dropped after the first three feature signals at the norms.
However, the thigh signals appeared to provide notably less information relevance in respect of the gait phase classification problem compared to the other limbs. In general, the absolute maximum angular velocities and accelerations at the thigh were significantly smaller with less pronounced characteristic points compared to the foot, cf. Fig. 5.

3.2 SVM Gait Phase Classification

We trained four different SVM classifiers on the same previously mentioned feature subsets, using a cross-validation approach to learn and test. To this end, eleven subjects were selected for training and a single one for testing, i.e. a leave-one-subject-out cross validation. The look-back window was defined as half a second ($N=30$ samples) in all cases. For each limb segment and every feature set we evaluated the gait events in terms of precision $p = t_p/(t_p + f_p)$ and recall $r = t_p/(t_p + f_n)$ with t_p, f_p the true and false positives and f_n the false negatives. Additionally, we reported a recall-10 rate, which accepted only those predictions that were at maximum 10 frames away from the ground truth events. Moreover, the mean and standard deviation of the absolute frame lags between classified and true events were computed. A lag of one corresponds to a time delay of $16.\bar{6}$ ms due to the sampling rate of our setup. All results are summarized in Tab. 1.

		precision	recall	recall-10	abs. lags
Foot					
HS	$\omega_y^{S_\omega}$	0.772	1.000	0.992	2.91 / 1.72
	f	0.942	1.000	0.997	1.48 / 1.51
	$\bar{f}$	0.978	1.000	1.000	1.28 / 1.18
	$\|\|a\|\|_2$, $\|\|\omega\|\|_2$	0.903	1.000	0.995	1.80 / 2.02
TO	$\omega_y^{S_\omega}$	0.778	1.000	1.000	1.33 / 1.21
	f	0.949	1.000	1.000	1.08 / 0.91
	$\bar{f}$	0.984	1.000	1.000	1.16 / 0.96
	$\|\|a\|\|_2$, $\|\|\omega\|\|_2$	0.907	1.000	0.996	1.59 / 1.17
Shank					
HS	$\omega_y^{S_\omega}$	0.726	1.000	0.998	2.96 / 1.72
	f	0.907	1.000	0.999	1.59 / 1.46
	$\bar{f}$	0.941	1.000	1.000	1.42 / 1.30
	$\|\|a\|\|_2$, $\|\|\omega\|\|_2$	0.716	1.000	0.979	1.71 / 2.09
TO	$\omega_y^{S_\omega}$	0.730	1.000	0.999	3.01 / 1.50
	f	0.912	1.000	0.997	1.14 / 1.11
	$\bar{f}$	0.946	1.000	0.998	1.14 / 1.04
	$\|\|a\|\|_2$, $\|\|\omega\|\|_2$	0.723	1.000	0.996	1.65 / 1.39
Thigh					
HS	$\omega_y^{S_\omega}$	0.938	1.000	0.944	3.29 / 2.44
	f	0.887	1.000	0.972	2.31 / 2.15
	$\bar{f}$	0.890	1.000	0.980	2.10 / 2.03
	$\|\|a\|\|_2$, $\|\|\omega\|\|_2$	0.455	1.000	0.849	3.80 / 2.99
TO	$\omega_y^{S_\omega}$	0.946	1.000	0.988	1.58 / 1.39
	f	0.895	1.000	0.989	1.44 / 1.45
	$\bar{f}$	0.898	1.000	0.989	1.38 / 1.45
	$\|\|a\|\|_2$, $\|\|\omega\|\|_2$	0.478	1.000	0.923	2.13 / 2.60

legend

$1.00 > v \geq 0.99$	$0.99 > v \geq 0.90$	$0.90 > v \geq 0.80$	$0.80 > v$

Table 1. Gait phase detection results for a SVM classifier with a linear kernel.

For every feature set and event the recall rate was 1.0, meaning that no false negatives occurred within the test data set in any setup.
A classifier considering only the sagittal angular velocity $\omega_y^{S_\omega}$ showed recall-10 rates consistently over 0.94. The precision rates for the foot and shank were below 0.8 and therefore belonged to the worst among all features. For the thigh, instead, the precision was superior compared to the remaining feature sets.
From foot to the thigh, the recall-10 dropped for the HS from 0.992 to 0.944 and for the TO from 1.0 to

0.988. This is in accordance to the mRMR scores for the sagittal angular velocity, which showed decreasing feature relevance as limbs further away from the ground were considered.

4. DISCUSSION

The three proposed feature signals f yielded consistently high precision and recall rates and reduced absolute lags, which indicates that the acceleration signals provide valuable additional information. Regarding the absolute lags, using angular velocity only caused the biggest delay, i.e. temporal detection uncertainty, w.r.t. to the ground truth events at the foot and shank.
The extended feature set $\bar{f}$ showed the best performance for each segment and events. In terms of the precision, it outperformed the three feature signals marginally, while the additional benefits were rather low. The recall-10 rates of $\bar{f}$ and f were equally high.
The feature set of the signal norms $||a||_2, ||\omega||_2$, containing no directional information, performed comparably poor overall, which is in accordance with the evidence of the mRMR scoring. At both shank and thigh the precision dropped considerably and in case of the thigh also the recall-10 rates decreased markedly.

The proposed gait feature signals provide intuitive and predictive gait features, which are considerably more informative for segmentation tasks, when compared to commonly used signals, such as norms of acceleration and angular velocity data.
The classifier-independent mRMR feature ranking clearly emphasized the advantages of the directional information in the sagittal feature signals and especially showed the importance of the sagittal angular velocity. The vertical and anteroposterior accelerations still provide valuable additional information in terms of the precision and timeliness of event predictions, whereas norm signals were consistently ranked last.
Reliable gait phase segmentation, using inertial data, appears to become more challenging as the sensor is mounted farther away from the foot, being the limb, where events immediately emerge. While for foot and thigh the differences were minor, the relevance of the first selected feature, namely the sagittal angular velocity, dropped considerably in case of the thigh.
In any case, we were still able to detect the TO and HS events reliably in an online scenario. Applying a simple linear SVM classifier on the proposed feature signals, yielded high precision and high to excellent recall rates for any lower limb segment, even at the thigh. Note, that we did not smooth the transformed raw data in any way and the precision rates are likely to increase if spurious phase transitions related to the formulation of the classification problem can be avoided.

5. CONCLUSIONS AND OUTLOOK

Our approach is real-time capable, invariant of any prior knowledge, regarding the sensor mounting orientation and can be computed without the use of magnetometers. We extracted explicit feature signals from an IMU attached to any lower limb segment, using the same consistent method: Raw accelerometer and gyroscope measurements were transformed into a favorable coordinate frame and continuously compensated for inclination changes, which allows to directly measure the sagittal information, particularly relevant during gait.
The resulting feature signal curves are biomechanically interpretable with characteristic points at the events of interest, cf. Fig. 5. Especially in case of the foot and shank, a more fine-grained gait segmentation including, f.i. foot-flat and heel-off events, appears to be attainable.

There are several possibilities of further improvements and applications in different contexts. Regarding the gait phase segmentation task, the classification approach could be changed or improved, ranging from non-linear kernels of the SVM, applying other classification approaches like k-nearest neighbors, decision trees, Gaussian processes or ensemble / boosting variants, to additional implicit feature extractors like neural networks with one of their deep variants. Moreover, the currently fixed look-back window might need adaptions, if the motion speed or style varies considerably and additional smoothing of the feature signals or the class predictions might further improve the classification robustness.
The features could certainly be used for other tasks at the lower limbs, like activity recognition or automatic detection of the sensor mounting orientation, i.e. the sensor-to-segment alignment implicitly computed with our approach, during the initial one-step calibration.
An extension to the pelvis or even the upper body segments, however, is not straight forward, since the predominant changes in motion are not necessarily constrained to the sagittal plane. In case of the pelvis, a similar approach is conceivable, including the angular velocity around the anteroposterior axis to distinguish the gait events of both legs.
Deeper investigations should be undertaken in order to evaluate the robustness of the feature signals under challenging conditions, such as walking in sharper curves and on inclined or uneven terrain.
Future work will evaluate the proposed method applied to pathological gait data of patients, suffering from lingering musculoskeletal restrictions after total hip arthroplasty, cf. Teufl et al. (2019).

ACKNOWLEDGEMENTS

The project has received funding from the Federal Ministry of Education and Research under grant agreement No 02L17C012 and from the European Union's Horizon 2020 research and innovation programme under grant agreement No 826304.

REFERENCES

Abhayasinghe, N. and Murray, I. (2014). Human gait phase recognition based on thigh movement computed using IMUs. In *2014 IEEE Ninth International Conference on Intelligent Sensors, Sensor Networks and Information Processing (ISSNIP)*, 1–4. doi: 10.1109/ISSNIP.2014.6827604.

Aminian, K., Najafi, B., Büla, C., Leyvraz, P.F., and Robert, P. (2002). Spatio-temporal parameters of gait measured by an ambulatory system using miniature gyroscopes. *Journal of Biomechanics*, 35(5), 689–699. doi:10.1016/S0021-9290(02)00008-8.

Aung, M.S.H., Thies, S.B., Kenney, L.P.J., Howard, D., Selles, R.W., Findlow, A.H., and Goulermas, J.Y. (2013). Automated Detection of Instantaneous Gait Events Using Time Frequency Analysis and Manifold Embedding. *IEEE Transactions on Neural Systems and Rehabilitation Engineering*, 21(6), 908–916. doi: 10.1109/TNSRE.2013.2239313.

Blum, A.L. and Langley, P. (1997). Selection of relevant features and examples in machine learning. *Artificial Intelligence*, 97(1), 245–271. doi:10.1016/S0004-3702(97)00063-5.

Bötzel, K., Marti, F.M., Rodríguez, M.Á.C., Plate, A., and Vicente, A.O. (2016). Gait recording with inertial sensors – How to determine initial and terminal contact. *Journal of Biomechanics*, 49(3), 332–337. doi: 10.1016/j.jbiomech.2015.12.035.

Caldas, R., Mundt, M., Potthast, W., Buarque de Lima Neto, F., and Markert, B. (2017). A systematic review of gait analysis methods based on inertial sensors and adaptive algorithms. *Gait & Posture*, 57, 204–210. doi: 10.1016/j.gaitpost.2017.06.019.

Cover, T.M. (1974). The best two independent measurements are not the two best. *IEEE Transactions on Systems, Man, and Cybernetics*, SMC-4(1), 116–117. doi:10.1109/TSMC.1974.5408535.

Ding, C. and Peng, H. (2005a). inimum redundancy feature selection frommicroarray gene expression data. *Journal of bioinformatics and computational biology*, 3(2), 185–205.

Ding, C. and Peng, H. (2005b). Minimum Redundancy Feature Selection from Microarray Gene Expression Data. *Journal of Bioinformatics and Computational Biology*, 3(2), 185–205.

Figueiredo, J., Santos, C., and Moreno, J. (2018). Automatic recognition of gait patterns in human motor disorders using machine learning: A review. *Medical Engineering & Physics*, 53. doi: 10.1016/j.medengphy.2017.12.006.

Guenterberg, E., Yang, A., Ghasemzadeh, H., Jafari, R., Bajcsy, R., and Sastry, S. (2009). A Method for Extracting Temporal Parameters Based on Hidden Markov Models in Body Sensor Networks With Inertial Sensors. *IEEE Transactions on Information Technology in Biomedicine*, 13(6), 1019–1030. doi: 10.1109/TITB.2009.2028421.

Gustafsson, F. (2012). *Statistical Sensor Fustion*. Studentlitteratur.

Jolliffe, I.T. (2002). *Principal Component Analysis*. Springer Series in Statistics. Springer-Verlag, New York, 2 edition. doi:10.1007/b98835.

Kim, J.N., Ryu, M.H., Yang, Y.S., and Hong, J.Y. (2014). Estimation of Walking Direction Estimation using a Shoe-mounted Acceleration Sensor. *International Journal of Multimedia and Ubiquitous Engineering*, 9(5), 215–222. doi:10.14257/ijmue.2014.9.5.21.

Kotiadis, D., Hermens, H.J., and Veltink, P.H. (2010). Inertial Gait Phase Detection for control of a drop foot stimulator: Inertial sensing for gait phase detection. *Medical Engineering & Physics*, 32(4), 287–297. doi: 10.1016/j.medengphy.2009.10.014.

Mannini, A., Genovese, V., and Maria Sabatini, A. (2014). Online Decoding of Hidden Markov Models for Gait Event Detection Using Foot-Mounted Gyroscopes. *IEEE Journal of Biomedical and Health Informatics*, 18(4), 1122–1130. doi:10.1109/JBHI.2013.2293887.

Maqbool, H.F., Husman, M.A.B., Awad, M.I., Abouhossein, A., Iqbal, N., and Dehghani-Sanij, A.A. (2017). A Real-Time Gait Event Detection for Lower Limb Prosthesis Control and Evaluation. 25(9), 1500–1509. doi:10.1109/TNSRE.2016.2636367.

Mariani, B., Rouhani, H., Crevoisier, X., and Aminian, K. (2013). Quantitative estimation of foot-flat and stance phase of gait using foot-worn inertial sensors. *Gait & Posture*, 37(2), 229–234. doi: 10.1016/j.gaitpost.2012.07.012.

Perry, J. and Burnfield, J. (2010). *Gait Analysis: Normal and Pathological Function*. SLACK INC, Thorofare, NJ, 002 edition.

Rueterbories, J., Spaich, E.G., and Andersen, O.K. (2014). Gait event detection for use in FES rehabilitation by radial and tangential foot accelerations. *Medical Engineering & Physics*, 36(4), 502–508. doi: 10.1016/j.medengphy.2013.10.004.

Schicketmueller, A., Rose, G., and Hofmann, M. (2019). Feasibility of a Sensor-Based Gait Event Detection Algorithm for Triggering Functional Electrical Stimulation during Robot-Assisted Gait Training. *Sensors*, 19(21), 4804. doi:10.3390/s19214804.

Seel, T., Landgraf, L., Cermeño Escoba, V., and Schauer, T. (2014). Online Gait Phase Detection with Automatic Adaption to Gait VelocityChanges Using Accelerometers and Gyroscopes. *Biomedical Engineering / Biomedizinische Technik*, 59(Supplement), 758–909. doi: 10.1515/bmt-2014-5011.

Storm, F.A., Buckley, C.J., and Mazzà, C. (2019). Gait event detection in laboratory and real life settings: Accuracy of ankle and waist sensor based methods. 50, 42–46. doi:10.1016/j.gaitpost.2016.08.012.

Taborri, J., Rossi, S., Palermo, E., Patanè, F., and Cappa, P. (2014). A Novel HMM Distributed Classifier for the Detection of Gait Phases by Means of a Wearable Inertial Sensor Network. *Sensors*, 14(9), 16212–16234. doi:10.3390/s140916212.

Teufl, W., Taetz, B., Miezal, M., Lorenz, M., Pietschmann, J., Jöllenbeck, T., Fröhlich, M., and Bleser, G. (2019). Towards an inertial sensor-based wearable feedback system for patients after total hip arthroplasty: Validity and applicability for gait classification with gait kinematics-based features. *Sensors*, 5006(22).

Vinh, L.T., Thang, N.D., and Lee, Y.K. (2010). An improved maximum relevance and minimum redundancy feature selection algorithm based on normalized mutual information. *2010 10th IEEE/IPSJ International Symposium on Applications and the Internet*, 395–398.

Wang, Z., Zhao, H.Y., Qiu, S., and Gao, Q. (2015). Stance-Phase Detection for ZUPT-Aided Foot-Mounted Pedestrian Navigation System. *IEEE/ASME Transactions on Mechatronics*, 20, 1–1. doi: 10.1109/TMECH.2015.2430357.

Wikimedia Commons (2014). The free media repository. Anatomical Planes.

Zhao, Z., Anand, R., and Wang, M. (2019). Maximum relevance and minimum redundancy feature selection methods for a marketing machine learning platform.